Electric Power Systems Research 81 (2011) 974–983

Electric Power Systems Research

journal homepage: www.elsevier.com/locate/epsr

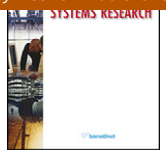

Visualizing time-varying harmonics using filter banks

Carlos Augusto Duque[a,*], Paulo M. Silveira[b], Paulo F. Ribeiro[c]

[a] Federal University of Juiz de Fora, Brazil
[b] Federal University of Itajubá, Brazil
[c] Calvin College, USA & Federal University of Juiz de Fora, Brazil

ARTICLE INFO

Article history:
Received 30 May 2009
Received in revised form 10 March 2010
Accepted 30 November 2010
Available online 22 December 2010

Keywords:
Harmonic distortion
Harmonic decomposition
Filter banks
Time-varying power harmonic distortion
Multi-resolution analysis
Wavelet transform

ABSTRACT

Although it is well known that Fourier analysis is in reality only accurately applicable to steady state waveforms, it is a widely used tool to study and monitor time-varying signals, such as are commonplace in electrical power systems. The disadvantages of Fourier analysis, such as frequency spillover or problems due to sampling (data window) truncation can often be minimized by various windowing techniques, but they nevertheless exist. This paper demonstrates that it is possible to track and visualize amplitude and time-varying power systems harmonics, without frequency spillover caused by time–frequency techniques. This new tool allows for a clear visualization of time-varying harmonics, which can lead to better ways to track harmonic distortion and understand time-dependent power quality parameters. It also has the potential to assist with control, protection and power quality applications.

1. Introduction

While estimation technique is concerned with the process used to extract useful information from the signal, such as amplitude, phase, and frequency, signal decomposition is concerned with the way that the original signal can be split in other components, such as harmonics, interharmonics, sub-harmonics, wavelet scale, etc.

Harmonic decomposition of a power system signal (voltage or current) is an important issue in power quality analysis. There are at least three reasons to focus on harmonic decomposition instead of harmonic estimation: (a) if separation of the individual harmonic component from the input signal can be achieved, the estimation task becomes easier; (b) the decomposition is carried out in the time-domain, such that the time-varying behavior of each harmonic component is observable; (c) time-varying harmonic decomposition can be used as input to a power quality event classifier, load identifier, power monitoring of time-varying harmonics and even some system protection applications.

Some existing techniques can be used to separate frequency components. For example, Short Time Fourier Transform (STFT) and Wavelets Transforms [1], are two well-known decomposition techniques. Both can be seen as a particular case of filter bank theory [2]. The STFT uses a filter with non-real coefficients, which generates a complex output signal whose magnitude corresponds to the amplitude of the harmonic component into the band. The main disadvantage of this method is the difficulty with the construction of an efficient band-pass filter with lower frequency spillover. Though wavelet transform uses filters with real coefficients, but the filters related with common wavelet mothers do not have good magnitude response in order to prevent frequency spillover. Additionally, the traditional binary tree structure is not able to divide the spectrum conveniently for harmonic decomposition and Discrete Wavelet Packet must be chosen in order to obtain a fair decomposition.

The adaptive notch filter and the phase-locked loop (PLL) [3,4] have been used for extracting time-varying harmonics components. However, the methods only work well in the case where a few harmonics components are present at the input signal. In other cases, the energies of adjacent harmonics spillover each other and the decomposed signal becomes contaminated. A similar approach as [3,4] was proposed in [5] where an adaptive filter-bank, labeled the resonator-in-a-loop filter bank, was used to track and estimate voltage or current harmonic signal in the power system. This paper only presents cases with odd harmonic tracking, and the non-stationary example presented deals just with the case of time varying frequencies.

In [6], the authors presented a technique based on multistage implementation of narrow low-pass digital filters to extract stationary harmonic components. The technique uses a multirate approach for the filter implementation and must know the system frequency for the modulation stage. The order of the narrow low-pass filter is very high, and consequently the transient response

* Corresponding author.
E-mail address: carlos.duque@ufjf.edu.br (C.A. Duque).

0378-7796
doi:10.1016/j.epsr.2010.11.030

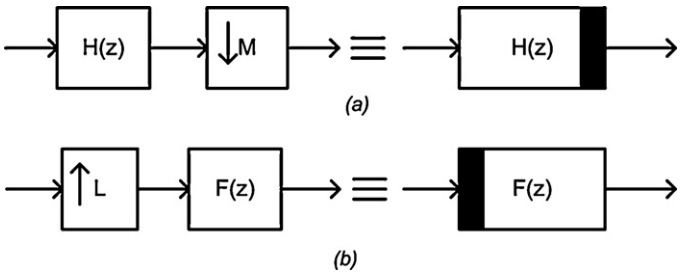

Fig. 1. Basic structures used in multirate filter bank and its equivalent representation for $L = M = 2$: (a) decimator; (b) interpolator.

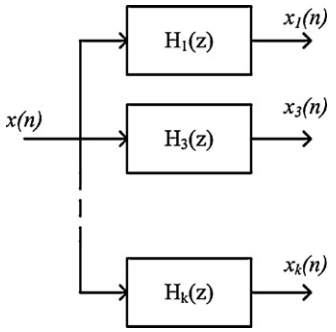

Fig. 2. Analysis bank filter to decomposed the input signal in its harmonics components.

time is long and the computational effort is substantial. No stationary example is presented in the paper.

Attempts to analyze time-varying harmonics using Wavelet Transform have been proposed in [7–9]. In [8,9] the analysis of non-stationary power system waveforms includes two steps. In the first step, the signal is decomposed into sub-bands using discrete wavelet packet transform (DWPT). In the second step, continuous wavelet transform (CWT) is applied to obtain the amplitude and phase of the harmonics. However, the methods are either computationally too complex or are not able to decouple the frequencies completely.

In [10], the authors have presented a new methodology to separate the harmonic components, until the 15th. It uses selected digital filters and down-sampling to obtain the equivalent band-pass filters centered at each harmonic. After the signal is decomposed by the analysis bank, each harmonic is reconstructed by using a synthesis bank structure. This structure is composed of filters and up-sampling that reconstructs each harmonic to its original sampling rate.

In this paper, the authors further explore the analytical basis and present new visualization forms for time-varying harmonics. It is worth to mention that the idea that harmonics should be treated as time-varying for short duration data window (few cycles) is very recent and implies breaking paradigms in the power systems community. The fact is that time-varying events, including harmonics, are now observed in the power system more often and therefore new tools to deal with them are demanded. Despite of the fact that the IEC 61000-4-7 considers harmonic as stationary signal, it is important to mention that IEC 61000-4-30, which is going through a review process is actually investigating the potential of such methods for time-varying harmonic measurements, for example during transformer energization events, etc.

The methodology presented in this paper might be promptly used for monitoring of time-varying individual power systems harmonics. Future applications may include control and protection functions, as well as interharmonic monitoring.

The paper is divided into method description, odd/even harmonic extraction, and simulation results.

2. Method description

Multirate systems employ a bank of filters with either a common input or summed output. The first structure is known as analysis filter bank [11,12] as it divides the input signal into different sub-bands in order to facilitate the analysis or the processing of the signal. The second structure is known as synthesis filter bank and is used if the signal needs to be reconstructed. Together with the filters, the multirate systems must include the sampling rate alteration operator (up- and down-sampling). Fig. 1 shows two basic structures used in a multirate system. Fig. 1(a) shows a decimator structure composed by a filter followed by the down-sampler device with a down sampling factor of M, and Fig. 1(b) the interpolator structure composed by a up-sampler (with an up-sampling factor of L) followed by a filter. The decimator structure is responsible to reduce the sampling rate by M, while the interpolator structure to increase it by L. At the right side of Fig. 1(a) simplified representations for the decimator and interpolator, used in this paper, when $M = L = 2$, is presented.

The direct way to build an analysis filter bank, in order to divide the input signal in its odd harmonic component, is represented in Fig. 2. In this structure $H_k(z)$ is the transfer function in the z domain of the kth band-pass filter centered at the kth harmonic and must be designed to have 3 dB bandwidth lower than $2f_0$, where f_0 is the fundamental frequency. If only odd harmonics are supposed to be present in the input signal, the 3 dB bandwidth can be relaxed to be lower than $4f_0$. Note that Fig. 2 is not a multirate system, because the structure does not include sampling rate alternation, which means that there is only one sampling rate in the whole system.

The practical problem concerning the structure shown in Fig. 2 is the difficulty to design each individual band-pass filter. This problem becomes more challenging when a high sampling rate must be used to handle the signal and the consequent abrupt transition band.

In this situation the best way to construct an equivalent filter bank is to use the multirate technique. Fig. 3 shows how an equivalent structure to Fig. 2 can be obtained by using the multirate approach. The filters $H_0(z)$ and $H_1(z)$ are quadrature mirror filters (QMF), designed using the power-symmetric approach [11], with the first one as a low-pass filter and the second a high-pass filter. At this point is useful to comment the difference between the QMF filters and typical wavelets filters, such Daubechies filters. The first difference is in the form that the high-pass filter is related with the low-pass filter. In QMF approach the relationship is given by $H_1(z) = H_0(-z)$ what implies that the impulse response of the $H_1(z)$ has alternating signs, meaning, $\{h_0(0), -h_0(1), h_0(2), -h_0(3)\ldots\}$, where $h_0(n)$ is the impulse response of $H0(z)$ [2]. In this case the magnitude of the high-pass filter is a mirror image of the magnitude of the low-pass filter with respect to the middle frequency. In the Daubechies filters the relationship is giving by $H_1(z) = -z^N \cdot H_0(-z)$ resulting in an alternating flip in the impulse response, $\{h_0(N), -h_0(N-1), h_0(N-2), -h_0(N-3)\ldots\}$. The second point is related with the way that the filters are generated. The QMF filter can be designed by using different techniques in frequency domain, being the power-symmetric approach used in this work. The wavelet filters are generated by using time domain especial function, proposed by the wavelet family creator. The simulations presented at this paper reveals that QMF filters are better choice for harmonic decomposition application than wavelet filters.

Fig. 4 shows the amplitude response for the analysis bank. This figure was obtained using a sampling rate equal to 64 samples per cycle and QMF FIR filters of 69th order, which contains 70 coefficients.

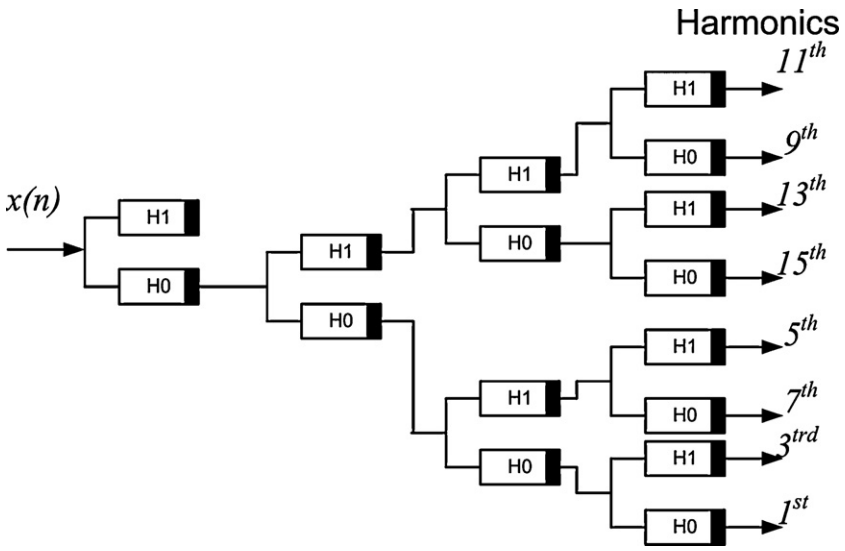

Fig. 3. Multirate equivalent structure to the filter bank in Fig. 2.

Note that the central frequency of each filter corresponds to the odd harmonic. Also the band-pass filters have poor rejection for even harmonics, so if they are present in the input signal they will mix up with even harmonics. Section 2.3 will focus on the way to eliminate even harmonics adding an extra IIR bandpass filter at each output on the analysis filter banks structure.

The main difference between the structure shown in Fig. 2, and the other one obtained by using the multirate technique, is the fact that the equivalent band pass filter is obtained by using only two QMF filter (low-pass and high-pass) and decimating operator. In fact, Fig. 3 can be represented by the equivalent filter bank shown in Fig. 5. The decimated signal at the output of each filter has a sampling rate 16 times lower then the input signal.

Note that the central frequency of each filter corresponds to the odd harmonic. Also the band-pass filters have poor rejection for even harmonics, so if they are present in the input signal they will mix up with even harmonics. Section 2.3 will focus on the way to eliminate even harmonics adding an extra IIR bandpass filter at each output on the analysis filter banks structure.

The equivalent filters $H_i(z)$, with $i = 1, 2 \ldots, k$, are obtained by using the noble identities for multirate systems [12]. These identities are shown in Fig. 6(a) and (b). The first identity shows that $H(z)$ must be changed to $H(z^M)$ when the down-sampling operator is moved from left to right. The second identity shows the reverse case.

Moving the down-sampling operators corresponding to the levels 1–3, in Fig. 3 to the right side of the level 4, and by using the noble identity 1, one can write, for example,

$$H1(z) = H_0(z) \cdot H_0(z^2) \cdot H_0(z^4) \cdot H_0(z^8) \quad (1)$$

and,

$$H7(z) = H_0(z) \cdot H_0(z^2) \cdot H_1(z^4) \cdot H_0(z^8) \quad (2)$$

Fig. 7 shows how the $H_7(z)$ magnitude response is obtained by using ideal QMF filters ($H_0(z)$ and $H_1(z)$). The frequency axis is normalized (1 correspond to $f_s/2 = 32f_0$, where f_s is the sampling frequency supposed to be $64f_0$). $H_i(z^k)$ ($i = 0$, 1 and $k = 1$, 2, 4 and 8) represent the periodic filter [10], whose periodicity is equal to $2\pi/k$. The intersection between all periodic filters (the cascade of them) results in the magnitude response of the equivalent multirate filter as illustrated in Fig. 5. In this example (Fig. 7) the intersection area ranges from [3/16 and 4/16] or in actual frequency between the 6th and 8th harmonic, and consequently has the central frequency at the 7th harmonic. This analysis explains why the third output (from the bottom up) in Fig. 3 corresponds to 7th harmonic instead of the 5th.

It is worth noting that the order of each harmonic in the bank corresponds to the well-known digital Gray code. The Gray code is binary numeral system where two successive values differ in only one digit. Table 1 shows the Gray code for four bits. Considering that

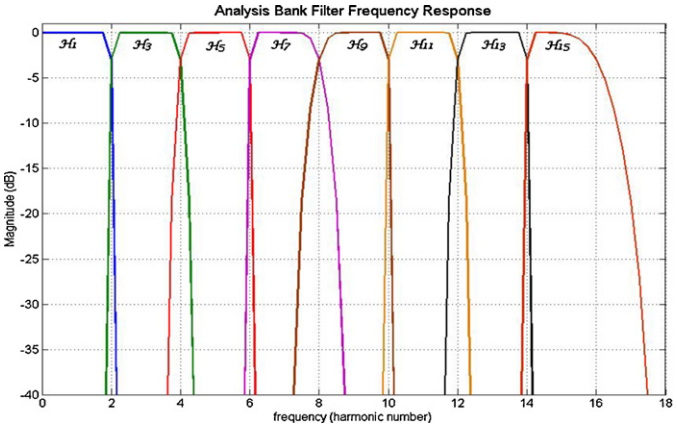

Fig. 4. Amplitude response in dB (frequency axis is labeled with the harmonic number).

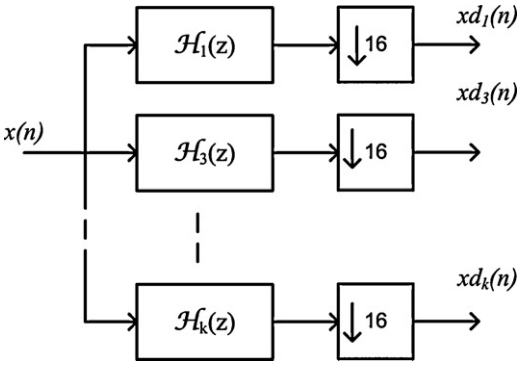

Fig. 5. Equivalent multirate analysis filter bank.

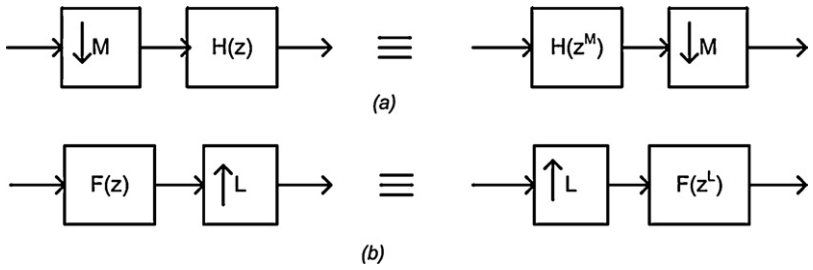

Fig. 6. Noble identities for multirate systems: (a) identity 1; (b) identity 2.

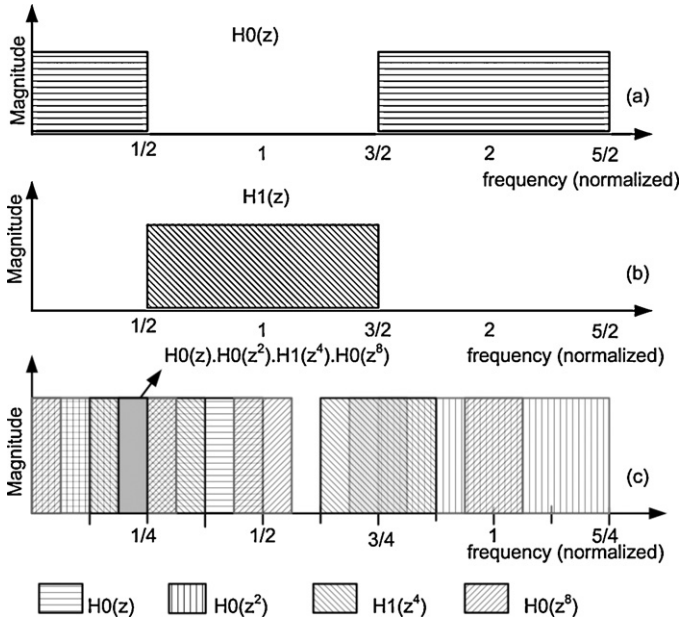

Fig. 7. Obtaining the equivalent magnitude response for $H_7(z)$. (a) $H_0(z)$ ideal magnitude response; (b) $H_1(z)$ ideal magnitude response; and (c) the equivalent magnitude response for $H7(z)$.

in this table "0" correspond to $H_0(z)$ and "1" correspond to $H_1(z)$, it is easy and practical to identify where each harmonic output is in Fig. 3. Despite of the fact that Fig. 3 shows the output of the first 15 odd harmonics, the extension for the first 30 odd harmonics is straight using this table.

2.1. The sampling frequency

In order to obtain the frequency response shown in Fig. 4 the sampling frequency used was 64 samples per cycle. This rate is related to the number of decomposition levels at the filter bank (Fig. 4 has 4 levels) through Eq. (3),

$$f_s = 2^{N+2} \cdot f_0 \tag{3}$$

Table 1
The gray code and corresponding harmonic output.

Gray code	Harmonic	Gray code	Harmonic
0000	1st	1100	17th
0001	3rd	1101	19th
0011	5th	1111	21st
0010	7th	1110	23rd
0110	9th	1010	25th
0111	11th	1011	27th
0101	13th	1001	29th
0100	15th	1000	31st

where f_0 is the power frequency and N is the number of decomposition levels. This sampling frequency was chosen in order that the cutoff frequency for each sub-band filter in Fig. 4 leads at the corresponding even harmonic frequency.

The highest odd harmonics that can be extracted by the filter bank is given by the Nyquist Theorem and is equal to $(2^{N+1} - 1)f_0$.

2.2. The downsampling effect

It is very important to understand what happens after the downsampling in Fig. 5. Depending on the harmonic component present at the output $Hk(z)$ it can become under-sampled. This is the case of the 7th harmonic in $H7(z)$, originally with 64 samples per cycle, and after a down-sampling operation, by a factor of 16, it will contain just 4 samples per cycle. In this case, this signal will appear at the output as a new sinusoidal signal with a different frequency as consequence of aliasing effect. This frequency is defined as an apparent frequency, f_a, and can be found through the equation given by [13],

$$f_a = \frac{\theta}{2\pi}\frac{f_s}{M} \tag{4}$$

where M is the downsampler factor and θ is the angle, in radians, obtained as show in [13].

Note that the 7th harmonic after downsampling will have the apparent frequency of 60 Hz, considering $f_s = 64f_0$ and $M = 16$. All other harmonics will result in the same apparent frequency of 60 Hz.

Fig. 8 shows the position of all harmonics after downsampling. Note that 60 Hz corresponds to the digital frequency of $\pi/2$ rad.

2.3. Filtering even harmonic

Fig. 8 shows the ideal situation when only one sinusoid is present inside of each filter band. However the frequency response of the filter bank (Fig. 4) shows that it is unable to filter the even component, so if an even component is present at the input signal the filter output will be polluted by this component. It is possible to show that all even harmonics, after downsampling, have apparent frequency equal to zero or π rad. In this way, a single second order band pass filter can be used to filter the even harmonics. Eq. (5) shows the transfer function of a typical second order parametric

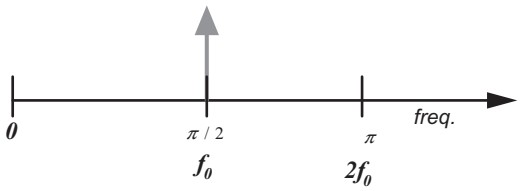

Fig. 8. Localization of harmonics component after down-sampling.

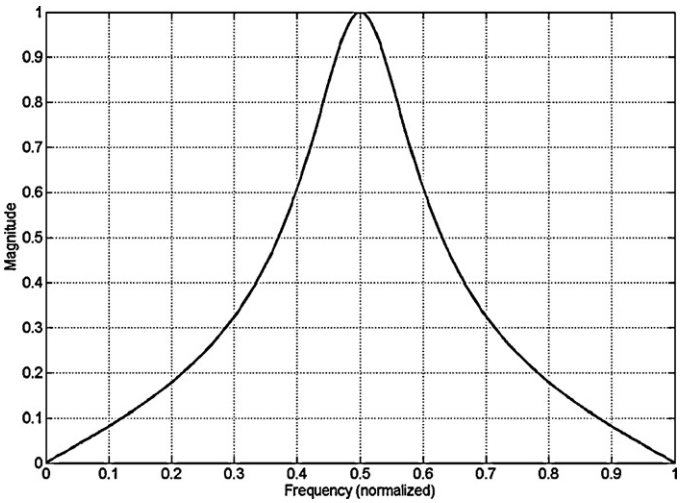

Fig. 9. Magnitude response of the IIR band pass filter used to filter even harmonics.

band-pass filter,

$$H_{BP}(z) = \frac{1-\alpha}{2}\frac{1-z^2}{1-\beta(1+\alpha)z^{-1}+\alpha z^{-2}} \quad (5)$$

In this equation, β defines the frequency where the filter has unitary gain and α defines the 3 dB bandwidth. Fig. 9 shows the magnitude response when $\alpha = 0.6$ and $\beta = \cos(\pi/2) = 0$. Note that this filter rejects the zero and π rad frequency components, and it has been used at the output of each stage at Fig. 3.

2.4. The synthesis filter banks

As described in Section 2.2, all harmonics at the output of the filter bank have the apparent frequency of f_0, sampled at a rate of 4 samples per cycle. One could use a single interpolator at this output to increase the sampling rate and improve the graphical resolution. However, this approach could not change the frequency to the original harmonic frequency. To reconstruct each harmonic into its original frequency, it is necessary to use the synthesis filter bank structure.

The synthesis filter bank, which has been used in this work, is not a conventional one. In the conventional synthesis filter bank the output of each previous level are added forming the inputs of the next level, in order that at the last level the original signal is reconstructed. As the objective is to reconstruct each harmonic instead of the original signal, the filter bank must be implemented in cascade, in order to obtain the corresponding harmonic, according to Fig. 10. In this figure $xd_i(n)$ $i = 1, 3, 5, ..., k$ represents the signals came

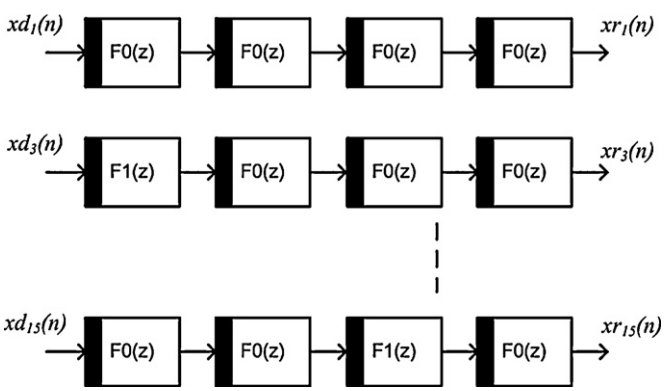

Fig. 10. Modified synthesis bank.

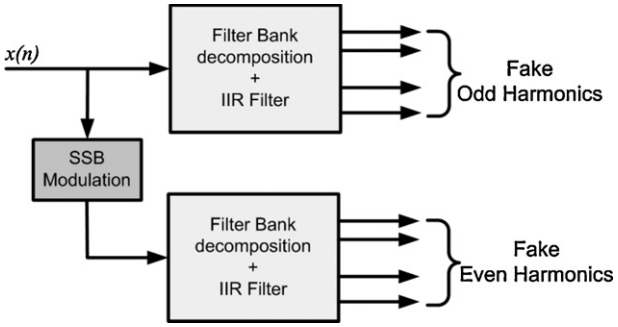

Fig. 11. Whole structure to harmonic extraction.

from the analysis filter bank and $xr_i(n)$ represents the harmonic components.

A practical way to obtain the cascade of reconstruction filters is to just invert the order of the Gray code in Table 1 and consider 0 as $F_0(z)$ and 1 as $F_1(z)$.

2.5. Extracting even harmonics

In order to extract the even harmonics the same bank can be used together with a preprocessing of the input signal. Hilbert transform is then used to implement a technique known as Single Side Band (SSB) modulation [11]. The SSB modulation moves to the right all frequencies in the input signal by f_0. In this way, even harmonics are changed to odd harmonics and vice versa. Fig. 11 shows the whole system for extracting odd and even harmonics.

3. Simulation results

In order to present some results of tracking time-varying harmonics using the structure shown in Fig. 11, four examples are considered: (a) a synthetic signal, which has been generated in Matlab using a mathematical model; (b) two signals obtained from the "Electromagnetic Transient Program including DC systems" (EMTDC) with its graphical interface known as "Power Systems Computer Aided Design" (PSCAD™); and (c) a real signal obtained from current acquired at the 88 kV side of the Aluminum Sheet Facility.

3.1. Synthetic signal

The synthetic signal utilized can be represented by:

$$x(t) = \sum_{h=1}^{N} A_h \sin(h\,\omega_0 t)\cdot f(t) + g(t) \quad (6)$$

where h is the order of the harmonic (1st up to 15th) and A_h is the magnitude of the respective component; ω_0 is the fundamental angular frequency; and finally, $f(t)$ and $g(t)$ are exponential functions (crescent, de-crescent or alternated one) or simply a constant value $\in \Re$. $x(t)$ is portioned in four different segments in such a way that the generated signal is distorted with some harmonics in steady-state and others varying in time, including abrupt and modulated change of magnitude and phase, as well as a DC component. Fig. 12 illustrates the synthetic signal.

The structure shown in Fig. 11 has been used to decompose the signal into sixteen different harmonic orders, including the fundamental (60 Hz) and the DC component.

Fig. 13 shows the decomposed signal from 4th up to 7th harmonic components. The left column represents the original components and the right column the corresponding components obtained through the filter bank. For simplicity and space limita-

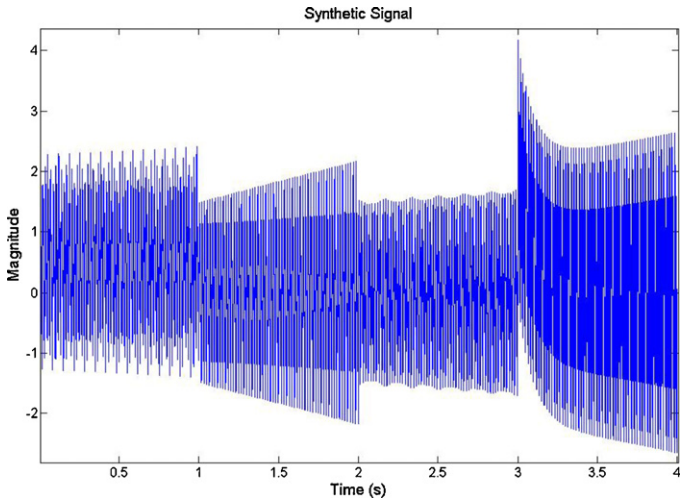

Fig. 12. Synthetic signal used.

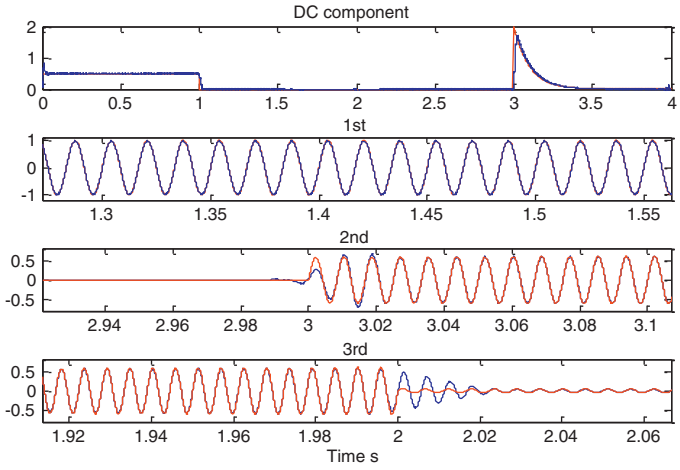

Fig. 14. Comparing original and decomposed component.

tion the other components are not shown. However, it is important to remark that all waveforms of the time-varying harmonics are extracted with efficiency along the time.

Naturally, intrinsic delays will be present during the transitions from the previous state to the new state. Furthermore, the filter banks will introduce a linear phase shift that can be found using Eq. (7), below [11]

$$T(z) = \frac{1}{K}\sum_{i=0}^{K} H_i(z)G_i(z) \tag{7}$$

where $H_i(z)$ and $G_i(z)$ are, respectively, the equivalent filters for the analysis and synthesis bank, obtained as (1) and (2). As the phase of $T(z)$ is linear the phase compensation for each harmonic can be obtained easily. Fig. 14 shows both the original and the estimated components (DC to 3rd harmonic) in a short time scale interval, after the phase compensation is applied.

Table 2 shows comparative results using different filters inside the structure, some of them using well-known wavelet filters. The comparative parameters used were the means of all errors computed for each harmonic individually. The individual errors used were the mean square error (MSE), mean square percentage error (MSE%) and mean absolute percentage error (MAE%) and the mean of the error for each harmonic was named MMSE, MMSE% and MMAE%, respectively. The first two cases use the 69th and 33rd order QMF filters, respectively and the other cases use respectively Meyer and Daubechies (30 dB) Wavelet filters which filters' order are respectively 101 and 59. Note that the QMF filter has the lowest error. The QMF 33rd order has better results than the Meyer and Daubechies with further advantage of lower computational effort.

Table 2
Comparative performance between several filters in the filter banks.

Filter based on	MMSE	MMSE%	MMAE%
QMF 69th order	2.088e−4	0.0209	0.38
QMF 33rd order	3.569e−4	0.0357	0.80
Meyer	7.717e−4	0.0717	1.33
30 dB	9.952e−4	0.0995	1.83

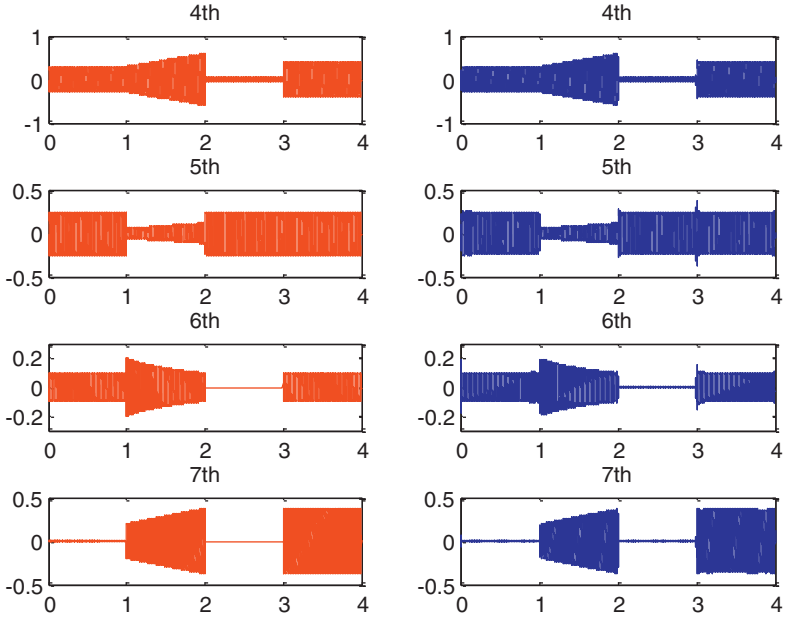

Fig. 13. First column: original components, second column: decomposed signals.

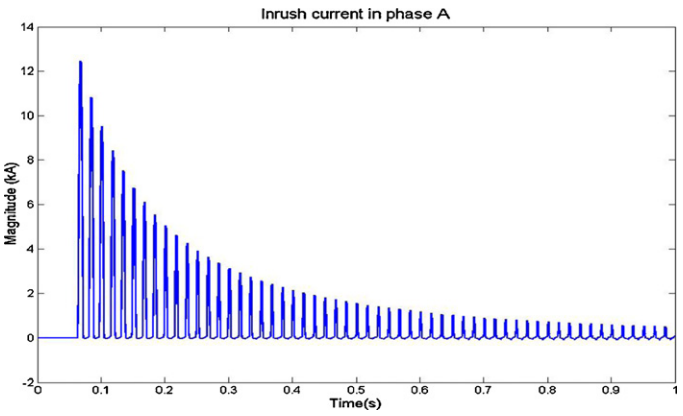

Fig. 15. Inrush current in phase A.

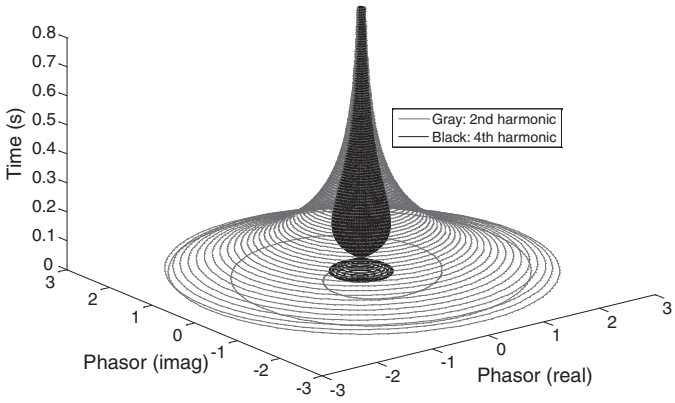

Fig. 17. The Impedance 3D polar plot for the 2nd and 4th harmonic (Inrush current).

3.2. Simulated signal

3.2.1. Inrush current example

It is well known that during energization a transformer can draw a large current from the supply system, normally called inrush current, whose harmonic content is high [14].

In recent years, improvements in materials and transformer design have lead to inrush currents with lower distortion content [15]. The magnitude of the second harmonic, for example, has dropped to approximately 7% depending on the design [16]. But, independent of these new improvements, it is always important to emphasize the time-varying nature of the inrush currents.

Therefore, a transformer energization case was simulated using EMTDC/PSCAD, and the result is shown in Fig. 15.

By using the methodology proposed to visualize the inrush current, Fig. 16 reveals the rarely seen time-varying behavior of the waveform of each harmonic component. This could be used to understand other physical aspects not observed previously. In Fig. 16, the left column shows the DC and even components and the right column the odd components.

Another way to visualize the dynamic behavior of each component is through the polar plot. To obtain the polar plot, the phasor of each component must be estimated. After the estimation, the real versus the imaginary part of the phasor are plotted. Fig. 17 shows the three-dimensional (3D) polar plot of the 2nd and 4th harmonics. By using this representation the time information is kept and so its time varying behavior.

3.2.2. Harmonic decomposition for six pulse converter

For medium and large power application, such as industrial drives, smelters, and HVDC transmission, the six-pulse bridge constitutes the basic converter unity. Theoretical studies [17] show that for ideal condition (no background distortion and no filtering) the current harmonic content is composed by the 5th, 7th, 11th, 13th, etc. components and are supposed time invariant. However in several situations the harmonics are time-varying as in the case of firing angle changes. Fig. 18 shows this behavior when the fire angle varies from 0 to 25° in a ramp shape. Note that the existence of such tools can lead to a new method to identify abnormal functioning of the converter, or in methodology to load identification.

3.3. Real signal

In the last example the current acquired at the 88 kV side of the aluminum sheet facility is analyzed. Fig. 19 shows the odd har-

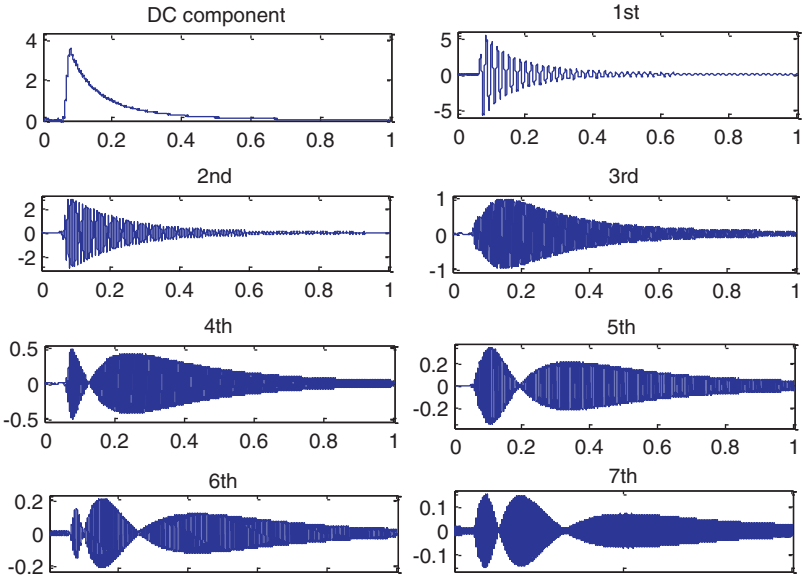

Fig. 16. Decomposition of the simulated transformer inrush current.

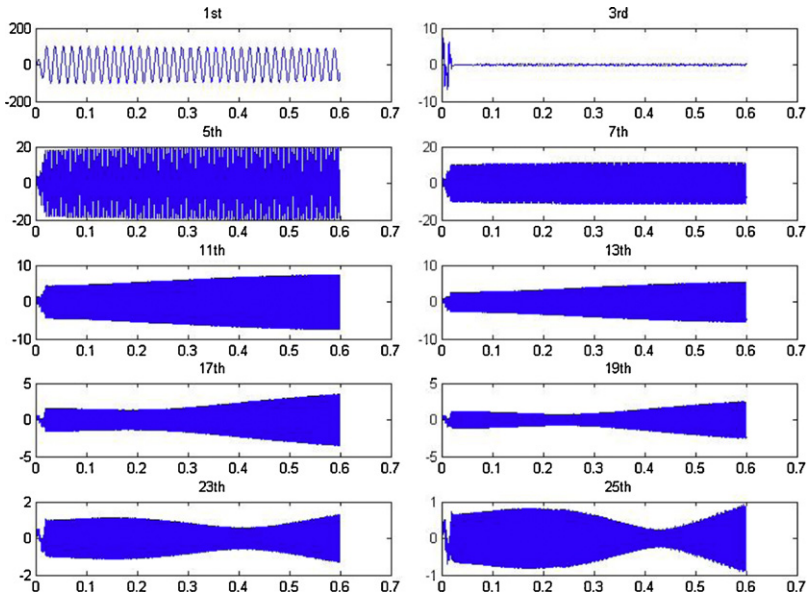

Fig. 18. Harmonic decomposition for six pulse converter (firing angle variation).

monic decomposition. Even decomposition is not shown because these components are not significant. Note that the components are time varying and the output corresponding to the 5th harmonic is the most significant component. It can be noted also from Fig. 19 that the third component seems to have the effect of beating, which identifies the presence of some interharmonic in this ouput. The same happens with the 7th, 9th, and 15th components.

Fig. 20 shows the spectrum of the current signal taking 12 cycles of the fundamental component and using rectangular window, as specified by the standard IEC61000-4-7, which results in a frequency resolution of 5 Hz. The figure shows the existence of several interharmonics lower than 5th harmonic. However the time dependency of each harmonic is not kept in this methodology.

Signal reconstruction is shown in Fig. 21, considering the odd and even components. Note that the reconstructed signal is closer to the real one; this means that the decomposition approach carries the main information of the whole signal.

4. Final consideration and future work

The methodology proposed has some intrinsic limitations associated with the analysis of interharmonics as well as with real time applications. Where they exist, the interharmonics are not filtered by the bank; they would corrupt the nearby harmonic components. The limitation regarding real time applications is related to the transient time response produced by the filter bank and the Hilbert Transformer implementation. Concerning the transient problem, the presence of abrupt change in the input signal, such

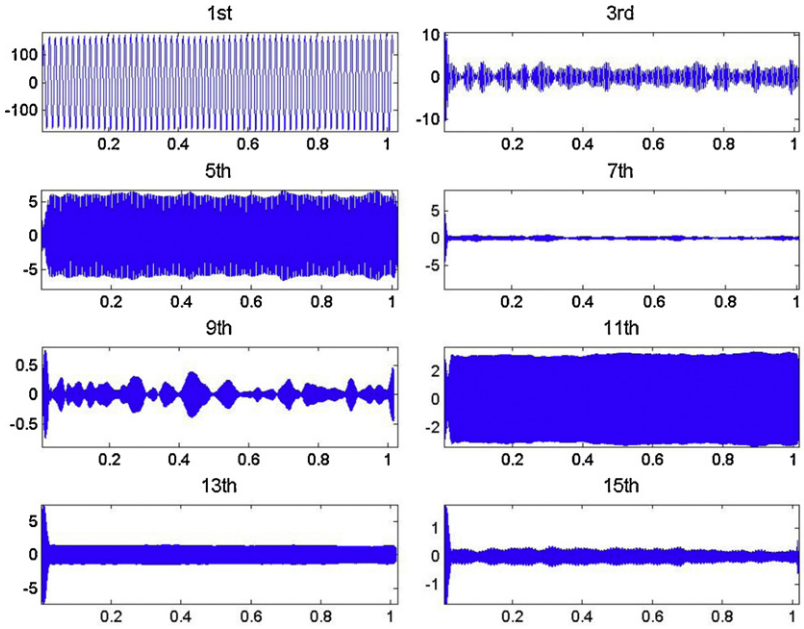

Fig. 19. Odd harmonic decomposition of current in aluminum sheet facility.

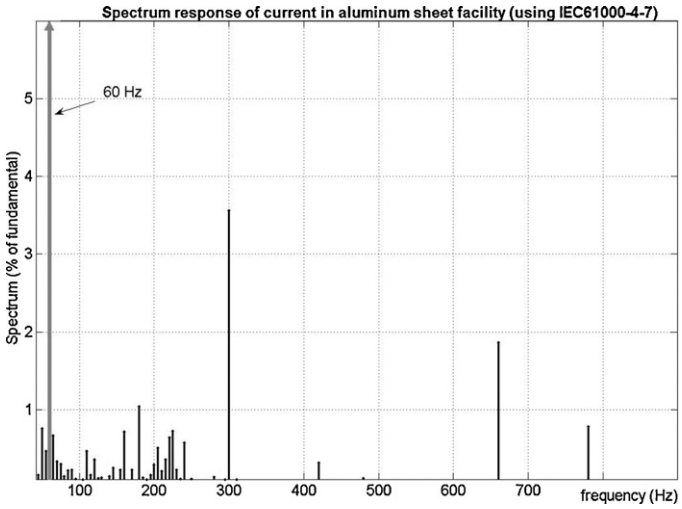

Fig. 20. Spectrum response of current in aluminum sheet facility, using IEC61000-4-7.

as in inrush currents, the transient response can last more than 5 cycles, which is not appropriate for applications whose time delay must be as short as possible. Concerning the Hilbert Transformer implementation, some filters used in the literature (mainly in communication area) do not produce good results and further research should address this problem. However for off-line or block processing application, the FFT based implementation leads to excellent results.

The computational effort for real time implementation is another challenge that the authors are investigating. In fact, the high order filter (69th) used in the bank structure demands high computational effort. By using multirate techniques to implement the structure it is possible to show that the number of multiplications per second to implement one branch of the analysis filter bank of Fig. 3 is about 250,000. Some low price Digital Signal Processors (DSPs) available in the market are able to execute 300 million float pointing operations per second. This shows that, despite the higher computational effort of the structure, it is feasible to be implemented in hardware. However, new opportunities exist for overcoming the limitations and the development of improved and alternative algorithms.

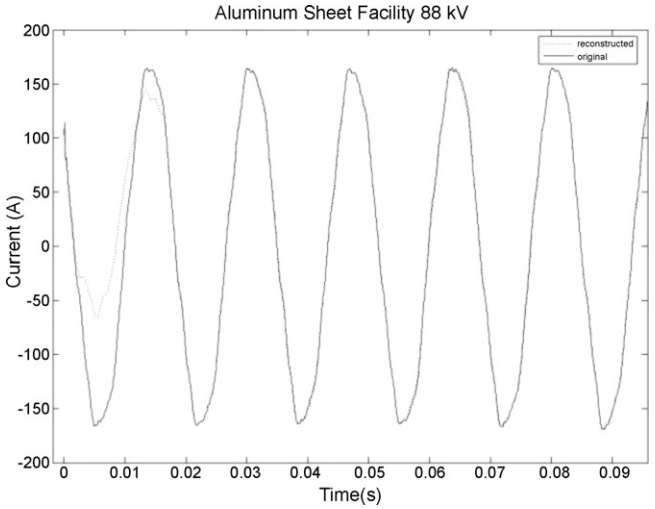

Fig. 21. The real and reconstruction signal (zoomed version).

5. Conclusions

This paper presents a new method for time-varying harmonic decomposition based on multirate filter banks theory. The technique is able to extract each harmonic in the time domain. The composed structure was developed to work with 256 samples per cycle and to track up to the 15th harmonic. The methodology can be adapted through convenient pre-processing for different sampling rates and higher harmonic orders.

The paper focused on the methodology for splitting the signal in time-varying harmonic component. Application of such methodology in analysis and synthesis problems of power system and industry needs more investigation, but the authors foreseen that it can be used in control, protection and power quality application. The IEC61000-30 is investigating the potential of such methods for time-varying harmonic measurements.

Acknowledgements

The authors would like to thanks Dr. Roger Bergeron and Dr. Mathieu van den Berh for their useful and constructive suggestions. The authors would like to thanks the Brazilian research agencies that supported this work: CNPq and FAPEMIG.

References

[1] Gu. Yuhua, M.H.J. Bollen, Time-frequency and time-scale domain analysis, IEEE Trans. Power Deliv. 15 (4) (2000) 1279–1284.
[2] G. Strang, T. Nguyen, Wavelets and Filter Banks, Wellesley-Cambridge Press, 1997.
[3] M. Karimi-Ghartemani, M. Mojiri, A.R. Bakhsahai, A technique for extracting time-varying harmonic based on an adaptive notch filter, in: Proc. of IEEE Conference on Control Applications, Toronto, Canada, 2005, pp. 624–628.
[4] J.R. Carvalho, P.H. Gomes, C.A. Duque, M.V. Ribeiro, A.S. Cerqueira, J. Szczupak, PLL based harmonic estimation, in: IEEE PES Conference, Tampa, FL, USA, 2007, pp. 1–6.
[5] H. Sun, G.H. Allen, G.D. Cain, A new filter-bank configuration for harmonic measurement, IEEE Trans. Instrum. Meas. 45 (3) (1996) 739–744.
[6] C.-L. Lu, Application of DFT filter bank to power frequency harmonic measurement, IEE Proc. Gener. Transm. Distrib. 152 (1) (2005) 132–136.
[7] P.M. Silveira, M. Steurer, P.F. Ribeiro, Using wavelet decomposition for visualization and understanding of time-varying waveform distortion in power system, in: VII CBQEE-Brazil, 2007, pp. 102–109.
[8] V.L. Pham, K.P. Wong, Antidistortion method for wavelet transform filter banks and nonstationary power system waveform harmonic analysis, IEE Proc. Gener. Transm. Distrib. 148 (2) (2001) 117–122.
[9] V.L. Pham, K.R. Wong, Wavelet-transform-based algorithm for harmonic analysis of power system waveforms, IEE Proc. Gener. Transm. Distrib. 146 (3) (1999) 249–254.
[10] C.A. Duque, P.M. Silveira, T. Baldwin, P.F. Ribeiro, Novel method for tracking time-varying power harmonic distortion without frequency spillover, in: IEEE 2008 PES, Pittsburgh, PA, USA, 2008, pp. 1–6.
[11] Sanjit K. Mitra, Digital Signal Processing – A Computer-based Approach, third ed., Mc-Graw Hill, 2006.
[12] P.P. Vaidyanathan, Multirate Systems and Filter Banks, Prentice Hall Signal Processing Series, 1993.
[13] J.R. Carvalho, C.A. Duque, M.V. Ribeiro, A.S. Cerqueira, P.F. Ribeiro, Time-Varying Harmonic Distortion Estimation Using PLL Based Filter Bank and Multirate Processing, VII CBQEE-Brazil, 2007. Available from: http://www.ufjf.br/pscope.
[14] C.R. Mason, The Art and Science of Protective Relaying, John Wiley & Sons, Inc., New York, 1956.
[15] B. Gradstone, Magnetic solutions, solving inrush at the source, Power Electron. Technol. April (2004) 14–26.
[16] F. Mekic, R. Girgis, Z. Gajic, E. Nyenhuis, Power transformer characteristics and their effect on protective relays, in: 33rd Western Protective Relay Conference, 2006.
[17] J. Arrilaga, B.C. Smith, N.R. Watson, A.R. Wood, Power Harmonic Analysis, John Wiley & Sons, 1997.

Carlos A. Duque was born in Juiz de Fora, Brazil, in 1962. He received the B.S. degree in Electrical Engineering from the Federal University of Juiz de Fora, Brazil, in 1986, and the M.Sc. and Ph.D. degree from the Catholic University of Rio de Janeiro, in 1990 and 1997, respectively, in Electrical Engineering. Since 1989 he is a Professor in the Engineering Faculty at Federal University of Juiz de Fora (UFJF), in Brazil. He is a Visiting Researcher at the Center for Advanced Power Systems (CAPS) at Florida State University, Tallahassee, Florida. His research interests are power quality analysis, digital instrumentation and digital signal processing.

Paulo Márcio da Silveira was born in Itajubá/MG, Brazil in 1960. He received his BSEE and M.Sc degrees from the Federal Engineering School of Itajubá (EFEI), Brazil, in 1984 and 1991, respectively, and his D.Sc degree in electrical engineering from University of Santa Catarina (UFSC), Brazil, in 2001. He is Associate Professor at Federal University of Itajubá, where he is also the Power Quality Study Group sub-coordinator. His interest areas are Power System Protection, Power Quality and Signal Processing for Instrumentation.

Paulo F. Ribeiro received a B.S. in Electrical Engineering from the Universidade Federal de Pernambuco, Recife, Brazil, completed the Electric Power Systems Engineering Course with Power Technologies, Inc. (PTI) 1, and received the Ph.D. from the University of Manchester, Manchester-UK. Presently, he is a Professor of Engineering at Calvin College, Grand Rapids, Michigan, on sabbatical at the Center for Advanced Power Systems (CAPS) at Florida State University, Tallahassee, Florida. Dr. Ribeiro is active in IEEE, CIGRE and IEC working groups on power quality. He is Registered Professional Engineer in the State of Iowa.